

Domain Decomposition Methods for Solving The Helmholtz Problem by High-Order Finite Element Methods

Youngjoon Cha* and Seongjai Kim†

ABSTRACT

An iterative domain decomposition method is considered for solving the Helmholtz wave equation by high-order quadrilateral finite element methods. The iteration is performed in a block Jacobi manner with a minimum overlap. For the interface operator, a Robin boundary condition is employed in a modified form which fits possible discontinuities of the normal components of the discrete flux on the subdomain interfaces. The algorithm is analyzed using energy estimates. Numerical results are given to show the effectiveness of the algorithm for the simulation of high-frequency waves in heterogeneous media in the two-dimensional space.

Key words. Helmholtz wave equation, domain decomposition method, quadrilateral finite element method, artificial damping iteration, quality factor.

AMS subject classifications. 65N55, 65F10.

*Department of Applied Mathematics, Sejong University, 98 Kunja-Dong, Seoul, 143-747, South Korea Email: yjcha@sejong.ac.kr

†Department of Mathematics, University of Kentucky, Lexington, Kentucky 40506-0027 USA Email: skim@ms.uky.edu. The work of this author is supported in part by NSF grant DMS-0312223.

1. INTRODUCTION

Wave propagation in real media such as the earth materials is affected by attenuation and dispersion. Therefore, a realistic simulation of wave propagation phenomena should be able to reproduce these two effects. Wave equations are often imposed by a suitable radiation condition at infinity. Such problems can be solved numerically by truncating the given unbounded domain, imposing a suitable absorbing boundary condition (ABC) on the boundary of the truncated bounded domain, approximating the resulting problem using discretization methods (e.g., finite differences and finite element methods), and applying computational algorithms to the resulting algebraic system.

In this paper, we will consider a domain decomposition (DD) method for solving the Helmholtz problem by finite element (FE) methods. Let $\Omega \subset \mathbb{R}^d$, $d = 2$ or 3 , be a logically rectangular/cubic domain with its boundary $\Gamma = \partial\Omega$. Consider the following Helmholtz problem

$$\begin{aligned} \text{(a)} \quad & -\Delta u - K(\mathbf{x})^2 u = S(\mathbf{x}), \quad \mathbf{x} \in \Omega, \\ \text{(b)} \quad & \frac{\partial u}{\partial \nu} + i\alpha(\mathbf{x}) u = 0, \quad \mathbf{x} \in \Gamma, \end{aligned} \tag{1.1}$$

where i is the imaginary unit, ν is the unit outward normal to Γ , and the coefficients $K(\mathbf{x})$ and $\alpha(\mathbf{x})$ satisfy

$$\begin{aligned} K(\mathbf{x})^2 &= p(\mathbf{x})^2 - iq(\mathbf{x})^2, \quad 0 < p_0 \leq p(\mathbf{x}) \leq p_1 < \infty, \quad 0 \leq q_0 \leq q(\mathbf{x}) \leq q_1 < \infty, \\ \alpha &= \alpha_r - i\alpha_i, \quad \alpha_r > 0, \quad \alpha_i \geq 0, \end{aligned}$$

and are sufficiently regular so that (1.1) admits a unique solution lying in $H^1(\Omega)$ for reasonable source S . The coefficient α is assumed to be properly chosen such that (1.1b) represents a first-order ABC that allows normally incident waves to pass out of Ω transparently [8]. The problem (1.1) models the propagation of time-harmonic waves such as electromagnetic waves, seismic waves, underwater acoustics, discretization of the time-dependent Schrödinger equation by implicit difference schemes, and inverse scattering problems.

The Helmholtz problem (1.1) is difficult to solve numerically, in particular, when $0 \leq q \ll p$. In addition to having a complex-valued solution, it is neither Hermitian symmetric nor coercive; as a consequence, most standard iterative methods either fail to converge or converge so slowly. In many applications (e.g., the geophysical wave simulation and seismic velocity inversion), it is often required to reproduce waves up to 20-50 wavelengths. It is known that second-order discretization methods need to select at least 6-8 points per wavelength ($2\pi/p$) for stability reasons [23, 31]. However, for high-frequency applications, one should choose at least 10-12 and 20-25 grid points per wavelength respectively for stability and accuracy reasons [10, 23, 31]. Thus the

algebraic system for the numerical solution of the Helmholtz problem becomes very huge for realistic applications, besides being poorly-conditioned. It is hard to solve the problem (1.1) either by a direct method due to its problem size or by an iterative algorithm because of its large condition number and difficulties on preconditioning. In this context, DD methods are attractive for such a poorly-conditioned large problem; DD methods can combine iterative methods at the interface level and direct algorithms at the subdomain level.

Concerning iterative numerical solvers for (1.1), we refer to Bayliss *et al.* [1], Elman and Ernst [15], and Freund [17] for the Krylov subspace algorithms, and Douglas *et al.* [10] for the ADI method, for constant coefficient problems. Després [9] analyzed a DD algorithm for (1.1) in a differential, rather than discrete, level; his analysis was indebted in Lions [28]. Kim [19, 20, 21, 22, 24] studied nonoverlapping DD methods for solving the Helmholtz problem by finite difference and linear FE methods, along with acceleration techniques for an improved convergence; see also [23]. DD methods incorporating overlapping subdomains and GMRES accelerations have been studied by Widlund and Keyes and their colleagues [4, 29]. The so-called *ray-cycle* MG method has been studied by Lee *et al.* [27].

For the simulation of high-frequency waves in heterogeneous media, Kim *et al.* [25] suggested the so-called high-frequency asymptotic decomposition method, in which the wavefield was decomposed into two parts (the phase and the cumulative amplitude) and the solution could be simulated by solving two easier-to-solve equations.

The main objective of this article is to construct and analyze a finite element DD iterative procedure that is computationally efficient. We will consider a minimum overlapping DD method which is equivalent to a nonoverlapping algorithm incorporating a Robin interface boundary condition (RIBC). Note that RIBCs impose the continuity of both the discrete solution u^h and the normal components of its flux on the subdomain interfaces, while most conforming FE methods admit discontinuities in the normal flux on the element interfaces; the RIBC should be modified appropriately. For DD methods different from one presented in this paper, see the review articles by Dryja and Widlund [13] and Le Tallec [26].

An outline of the paper is as follows. In the next section we review briefly the existence and uniqueness of the solution of the Helmholtz problem, properties of the numerical solution and difficulties in its simulation, and the shape (basis) functions of FE methods. In Section 3, an iterative DD algorithm is introduced on the minimum overlapped partition of the domain. The algorithm seeks exactly the same numerical solution as the background FE method; the iteration is performed in block Jacobi manner with a modified RIBC. Section 4 presents a convergence analysis for the algorithm, utilizing energy estimates, when the attenuation coefficient is positive, i.e., $q(\mathbf{x}) \geq q_0 > 0$. The analysis is partially indebted in Douglas *et al.* [11], where a

nonoverlapping DD method incorporating an RIBC was proposed for solving symmetric positive definite problems by mixed methods. Since most mixed methods allow the discrete solution u^h to be discontinuous on the element interfaces, the RIBC will produce error unless it is modified appropriately. As a modification, they introduced Lagrange multipliers on the subdomain interfaces to overcome the “flux conservation error”. However, the situation is quite different for conforming FE methods: the introduction of Lagrange multipliers on the subdomain interfaces does hardly make the resulting DD problem equivalent to the original discrete problem. Thus, we employ the technique of minimum overlap in order for the decomposed problem to solve the original discrete one *always*. In Section 5, the artificial damping iteration (ArtDI) of [21, 24] is applied for the cases: $q = 0$ or q is small. Section 6 gives numerical results to show the effectiveness of the DD algorithm accelerated by the ArtDI. The algorithm is tested for various choices in the frequency, the velocity, and the order of FE methods. It has been numerically verified that (1) the ArtDI makes the algorithm converge and faster, (2) the FE error converges in one-order higher for the shape functions of orders ≥ 2 (superconvergence), and (3) the FE method of second-order shape functions introduces one-order higher destruction in the numerical accuracy as the frequency increases. The last section includes conclusions and applications.

Throughout the paper, we use standard notation for the function spaces and their norms and inner products; e.g., $L^2(D)$ is the space of all functions f on some domain D such that

$$\int_D |f|^2 d\mathbf{x} < \infty,$$

and $(\cdot, \cdot)_D$ and $\|\cdot\|_{0,D}$ are the corresponding inner product and norm, respectively. Analogously, $H^m(D)$ is the usual m -th order Sobolev spaces on D with the norm $\|\cdot\|_{m,D}$ for a natural number m .

2. PRELIMINARIES

This section begins with a brief review for the existence and uniqueness of the weak solution of (1.1). Then, we present convergence properties for the FE solution of the Helmholtz problem, followed by difficulties arising in solving the corresponding algebraic system. We will also address shape (basis) functions for quadrilateral FE methods.

2.1. Existence and uniqueness of the solution

The weak formulation of (1.1) is given by seeking $u \in V = H^1(\Omega)$ such that

$$(\nabla u, \nabla v)_\Omega - (K^2 u, v)_\Omega + \langle i\alpha u, v \rangle_\Gamma = (S, v)_\Omega, \quad \forall v \in V, \quad (2.1)$$

where

$$(f, g)_\Omega = \int_\Omega f \bar{g} d\mathbf{x}, \quad \langle f, g \rangle_\Gamma = \int_\Gamma f \bar{g} d\sigma.$$

For a simpler presentation, we define the following bilinear form

$$\mathcal{L}(u, v; D) = (\nabla u, \nabla v)_D - (K^2 u, v)_D + \langle i\alpha u, v \rangle_{\partial D \cap \Gamma}, \quad D \subset \Omega.$$

We cite the following lemma.

Lemma 2.1. [12] *The weak formulation (2.1) of the Helmholtz problem admits a unique solution $u \in H^1(\Omega)$ for $S \in L^2(\Omega)$.*

2.2. The discrete solution

Given a subspace $V^h \subset V \cap Q_r^h$, where Q_r^h is the space of the r -th order splines corresponding to the set of finite elements \mathcal{T}_h , the FE approximation of the solution u of (2.1) is the function $u^h \in V^h$ such that

$$\mathcal{L}(u^h, v; \Omega) = (S, v)_\Omega, \quad \forall v \in V^h. \quad (2.2)$$

Let the approximation error $e^h = u - u^h$, where u is the solution of (2.1) and u^h is the solution of (2.2). It is known [2] that (2.2) has a unique solution $u^h \in V^h$ for $p^2 h$ sufficiently small and that

$$\|e^h\|_{0,\Omega} = \mathcal{O}(p^{r+2}h^{r+1}), \quad \|e^h\|_{1,\Omega} = \mathcal{O}(p^{r+1}h^r), \quad (2.3)$$

for certain classes of data f , e.g., $\|f\|_{r-1,\Omega} \leq C_r \|u\|_{0,\Omega}$, where C_r is independent of p .

The algebraic system for (2.2) can be written as

$$A\mathbf{u}^h = \mathbf{b}. \quad (2.4)$$

Here we will employ a *mass-lumping* quadrature rule in which the quadrature points coincide with the degrees of freedom, i.e., we will consider quadrature-based shape functions; see §2.3 for details.

The matrix A in (2.4) can be written as

$$A = A_1 + iA_2,$$

where A_1 and A_2 are symmetric and real-valued. Since we have employed quadrature-based shape functions for V^h , the mass matrix A_2 should be diagonal. Furthermore, the diagonal elements of A_2 are positive if and only if $q(\mathbf{x}) \geq q_0 > 0$.

It is extremely difficult to solve (2.4) for non-attenuate or slightly-attenuate waves. The attenuation coefficient q is negligible for certain cases, e.g. ocean acoustics and optical waves in a vacuum. For the case that $0 \leq q \ll p$, it has been verified that relaxation methods such as Jacobi and SOR iterations does not converge and that nonsymmetric conjugate gradient (CG)-type algorithms (GCR [14], GMRES [30], etc.) either converge very slowly or have possible breakdowns [1, 16, 18]. The existence of a convergent nonsymmetric CG-type algorithm for (2.4) is equivalent to the positive definiteness of A_2 [17, 18].

2.3. The shape functions

We close the section by considering the shape functions associated with quadrilateral finite elements in the two-dimensional (2D) space. Let L_{k+1} be the Legendre polynomial of degree $(k+1)$ that satisfies the three-term recurrence relation

$$L_{k+1}(x) = \frac{(2k+1)xL_k(x) - kL_{k-1}(x)}{k+1}, \quad x \in [-1, 1],$$

where $L_0(x) = 1$ and $L_1(x) = x$. Then, the quadrature-based shape functions of degree r on the reference interval $[-1, 1]$ read

$$\widehat{\varphi}_i(x) = \prod_{\substack{\ell=0 \\ \ell \neq i}}^r \left(\frac{x - \widehat{x}_\ell}{\widehat{x}_i - \widehat{x}_\ell} \right), \quad i = 0, 1, \dots, r, \quad (2.5)$$

where $\{\widehat{x}_i\}$ are the Legendre-Gauss-Lobatto points of degree r : $\widehat{x}_0 = -1$, $\widehat{x}_r = 1$, and \widehat{x}_i are the zeros of L'_r , $i = 1, 2, \dots, r-1$; see [5] for details. Associated with the Legendre-Gauss-Lobatto points, the weights for the numerical quadrature are

$$\widehat{w}_i(x) = \frac{2}{r(r+1)[L_r(\widehat{x}_i)]^2}, \quad i = 0, 1, \dots, r, \quad (2.6)$$

with which the integration is exact for $f \in \mathbf{P}_{2r-1}$ (\mathbf{P}_{2r-1} is the set of polynomials of degree $\leq (2r-1)$), i.e.,

$$\int_{-1}^1 f(x) dx = \sum_{i=0}^r f(\widehat{x}_i) \widehat{w}_i, \quad \forall f \in \mathbf{P}_{2r-1}.$$

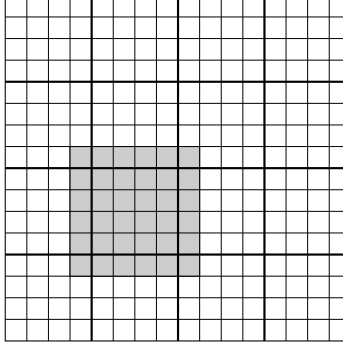
On the reference rectangle $[-1, 1]^2$, the shape functions of degree r , $\widehat{\varphi}_{ij}$, and associated weights \widehat{w}_{ij} are the tensor products defined as

$$\begin{aligned} \widehat{\varphi}_{ij}(x, y) &= \widehat{\varphi}_i(x) \widehat{\varphi}_j(y), \\ \widehat{w}_{ij} &= \widehat{w}_i \widehat{w}_j, \end{aligned} \quad i, j = 0, 1, \dots, r. \quad (2.7)$$

Then, for a quadrilateral finite element E , the corresponding shape functions $\{\varphi_{ij}\}$ are affine images of $\{\widehat{\varphi}_{ij}\}$ mapping from $[-1, 1]^2$ to E . See [7] for properties of such quadrature-based shape functions applied for FE methods.

3. THE DOMAIN DECOMPOSITION METHOD

In this section we introduce an iterative DD method, whose convergence will be analyzed in §4 under the assumption that $q \geq q_0 > 0$. In §5, we will address a remedy for the convergence for the general case: $q \geq 0$. For simplicity, consider 2D problems and choose a rectangular reference finite element with the shape functions being tensor products of 1D quadrature-based shape functions, as presented in §2.3.

Figure 1: The subdomain expansion $\tilde{\Omega}_j$ (shaded).

Thus the arguments to be presented are applicable to the 3D space with a minor change. Let \mathcal{T}_h be the set of finite elements in Ω which are affine images of the rectangular reference element and of which the largest edge length is no greater than h . Let V^h be the space of continuous piecewise polynomials (corresponding to \mathcal{T}_h) of order r for each coordinate variable.

3.1. Decomposition of the problem

Let $\{\Omega_j, j = 1, \dots, M\}$ be a nonoverlapping partition of Ω :

$$\bar{\Omega} = \bigcup_{j=1}^M \bar{\Omega}_j; \quad \Omega_j \cap \Omega_k = \emptyset, \quad j \neq k.$$

Assume that Ω_j are also logically rectangular regions sharing their interfaces with the finite elements in \mathcal{T}_h . Let

$$\Gamma_j = \Gamma \cap \partial\Omega_j, \quad \Gamma_{jk} = \Gamma_{kj} = \partial\Omega_j \cap \partial\Omega_k.$$

We expand each subdomain Ω_j into neighboring subregions by the element size h so that $\tilde{\Omega}_j \subset \Omega$. See Figure 1, where the bold lines indicate the interfaces of the original nonoverlapping subdomains. Let D^h be the sets of nodal points on \bar{D} , $D \subset \bar{\Omega}$, and $\tilde{\Gamma}_{jk} = \partial\tilde{\Omega}_j \cap \bar{\Omega}_k$. For function subspaces, let

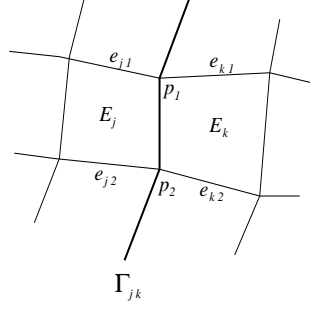
$$V_j^h = V^h|_{\Omega_j}, \quad V_{0,j}^h = \{v \in V_j^h : v|_{\Gamma_{jk}} = 0, \quad \forall k\}, \quad \tilde{V}_j^h = V^h|_{\tilde{\Omega}_j},$$

and $\tilde{V}_{I,j}^h$ be the set of functions in \tilde{V}_j^h that are possibly nonzero only on $\cup_k \Gamma_{jk}^h$ among all nodal points Ω^h . Set

$$\tilde{V}_{0,j}^h = V_{0,j}^h \bigoplus \tilde{V}_{I,j}^h.$$

For $\tilde{v}_j^h \in \tilde{V}_j^h$, we define (using subscripts in the same manner as in the definitions of subspaces)

$$v_j^h = \tilde{v}_j^h|_{V_j^h}, \quad v_{0,j}^h = \tilde{v}_j^h|_{V_{0,j}^h}, \quad \tilde{v}_{0,j}^h = \tilde{v}_j^h|_{\tilde{V}_{0,j}^h}, \quad \tilde{v}_{I,j}^h = \tilde{v}_j^h|_{\tilde{V}_{I,j}^h}. \quad (3.1)$$

Figure 2: A 2D mesh; $E_m \subset \Omega_m$, where $m = j, k$.

In the remainder of this section and the next section, the functions u_j^h , $u_{0,j}^h$, $\tilde{u}_{0,j}^h$, and $\tilde{u}_{I,j}^h$ should be considered as restrictions of \tilde{u}_j^h into the corresponding subspaces, if not specified. Also the same rule is employed for the test functions $\tilde{v}_j \in \tilde{V}_{0,j}^h$.

Decompose (2.2) over $\{\tilde{\Omega}_j\}$ as follows: find $\tilde{u}_j^h \in \tilde{V}_j^h$, $j = 1, \dots, M$, satisfying

$$\begin{aligned} \text{(a)} \quad & \mathcal{L}(\tilde{u}_j^h, \tilde{v}_j; \tilde{\Omega}_j) = (S, \tilde{v}_j)_{\tilde{\Omega}_j}, \quad \tilde{v}_j \in \tilde{V}_j^h, \\ \text{(b)} \quad & \tilde{u}_j^h = \tilde{u}_k^h, \quad \text{on } \tilde{\Omega}_j^h \cap \tilde{\Omega}_k^h. \end{aligned} \quad (3.2)$$

It can be easily verified that (3.2) has the same (unique) solution as (2.2) for $q \geq q_0 > 0$; each subproblem is well-posed for $q \geq q_0 \geq 0$ when it incorporates a Robin-type interface boundary condition, which we will impose to the resulting iterative procedure in a modified form; see (3.8) below. Note that we may choose the test function \tilde{v} in $\tilde{V}_{0,j}^h$ because of the essential boundary condition (3.2b).

3.2. Introduction of iterative procedure

We will first define a locally linear, continuous function $\sigma_{jk}(\mathbf{x})$ on Γ_{jk} , which is useful for the formulation of an iterative procedure for (3.2). See Figure 2. Let $E_m \subset \Omega_m$, $m = j, k$, be two elements sharing a portion of the interface Γ_{jk} . We denote the edges of the elements touching Γ_{jk} at a point by $e_{m,i}$, $m = j, k$, and the vertices by p_i , $i = 1, 2$, as in Figure 2. Then, σ_{jk} is defined on Γ_{jk} such that it is locally linear on each segment $\partial E_j \cap \partial E_k$ and its values on the corners are

$$\sigma_{jk}(p_i) = \frac{|e_{j,i}|}{|e_{j,i}| + |e_{k,i}|}, \quad i = 1, 2,$$

where $|e_{m,i}|$ denote the lengths of the edge $e_{m,i}$, $i = 1, 2$. (For example, $\sigma_{jk} \equiv 1/2$ for a uniform mesh of a rectangular domain.) Then, for $\tilde{v}_{I,j} \in \tilde{V}_{I,j}^h$,

$$\int_{E_j \cup E_k} \tilde{v}_{I,j} d\mathbf{x} = \int_{E_j} \tilde{v}_{I,j} d\mathbf{x} + \int_{E_k} \tilde{v}_{I,j} d\mathbf{x} \cong \int_{E_j} \frac{1}{\sigma_{jk}} \tilde{v}_{I,j} d\mathbf{x}, \quad (3.3)$$

where “ \cong ” means the equality in the numerical integration. It is not difficult to verify that the equality holds when the basis functions are tensor products of 1D

quadrature-based shape functions and the corresponding mass-lumping quadrature rule is employed for the numerical integration. (The adopted weights in the numerical quadrature are affine images of the reference weights related to the tensor product of Gauss-Lobatto points located on $[-1, 1]^2$. Thus they are scaled by the lengths of element edges.)

In the following we will view (3.2) as its corresponding algebraic system, if necessary. We now prove the following theorem.

Theorem 3.1. *The numerical solution of (3.2a) satisfies*

$$\begin{aligned} \mathcal{L}(\tilde{u}_j^h, \tilde{v}_j; \Omega_j) + (\nabla \tilde{u}_j^h, (\sigma_{jk} - 1) \nabla \tilde{v}_{I,j})_{\Omega_j} + \sum_k (\nabla \tilde{u}_j^h, \sigma_{jk} \nabla \tilde{v}_{I,j})_{\Omega_k} \\ = (S, \tilde{v}_j)_{\Omega_j}, \quad \tilde{v}_j \in \tilde{V}_{0,j}^h. \end{aligned} \quad (3.4)$$

Proof. Recall that $\tilde{v}_j = v_{0,j} + \tilde{v}_{I,j}$ for all $\tilde{v}_j \in \tilde{V}_{0,j}^h$. It follows from (3.2a) that

$$\begin{aligned} \text{(a)} \quad \mathcal{L}(\tilde{u}_j^h, v_{0,j}; \tilde{\Omega}_j) &= \mathcal{L}(\tilde{u}_j^h, v_{0,j}; \Omega_j) = (S, v_{0,j})_{\Omega_j}, \\ \text{(b)} \quad \mathcal{L}(\tilde{u}_j^h, \tilde{v}_{I,j}; \tilde{\Omega}_j) &= (S, \tilde{v}_{I,j})_{\tilde{\Omega}_j}. \end{aligned} \quad (3.5)$$

Equation (3.5b) in its algebraic system reads

$$(\nabla \tilde{u}_j^h, \sigma_{jk} \nabla \tilde{v}_{I,j})_{\tilde{\Omega}_j} - (K^2 \tilde{u}_j^h, \tilde{v}_{I,j})_{\Omega_j} + \langle i\alpha \tilde{u}_j^h, \tilde{v}_{I,j} \rangle_{\Gamma_j} = (S, \tilde{v}_{I,j})_{\Omega_j}, \quad \tilde{v}_{I,j} \in \tilde{V}_{I,j}^h, \quad (3.6)$$

where we have utilized the identity (at the algebraic level) presented in (3.3), i.e.,

$$\begin{aligned} (K^2 \tilde{u}_j^h, \tilde{v}_{I,j})_{\Omega_j} &= (K^2 \tilde{u}_j^h, \sigma_{jk} \tilde{v}_{I,j})_{\tilde{\Omega}_j}, \\ \langle i\alpha \tilde{u}_j^h, \tilde{v}_{I,j} \rangle_{\Gamma_j} &= \langle i\alpha \tilde{u}_j^h, \sigma_{jk} \tilde{v}_{I,j} \rangle_{\tilde{\Gamma}_j}, \\ (S, \tilde{v}_{I,j})_{\Omega_j} &= (S, \sigma_{jk} \tilde{v}_{I,j})_{\tilde{\Omega}_j}. \end{aligned}$$

Note that

$$\begin{aligned} \text{(a)} \quad (\nabla \tilde{u}_j^h, \sigma_{jk} \nabla \tilde{v}_{I,j})_{\tilde{\Omega}_j} &= (\nabla \tilde{u}_j^h, \sigma_{jk} \nabla \tilde{v}_{I,j})_{\Omega_j} + \sum_k (\nabla \tilde{u}_j^h, \sigma_{jk} \nabla \tilde{v}_{I,j})_{\Omega_k}, \\ \text{(b)} \quad (\nabla \tilde{u}_j^h, \nabla v_{0,j})_{\Omega_j} &= (\nabla \tilde{u}_j^h, \nabla \tilde{v}_j)_{\Omega_j} - (\nabla \tilde{u}_j^h, \nabla \tilde{v}_{I,j})_{\Omega_j}, \quad \tilde{v}_j \in \tilde{V}_{0,j}^h. \end{aligned} \quad (3.7)$$

(The reader should pay attention to the subscripts indicating the domain of integration.) Then, plug (3.7a) and (3.7b) respectively into (3.6) and (3.5a) and add the resulting equations to have (3.4). This completes the proof. \square

Now, we are ready to present the iterative DD algorithm for (3.2). For given initial guess $\tilde{u}_j^{h,0} \in \tilde{V}_j^h$, $j = 1, \dots, M$, find $\tilde{u}_j^{h,n} \in \tilde{V}_j^h$, $n \geq 1$, recursively by solving

the following system:

$$\begin{aligned}
\text{(a)} \quad & \mathcal{L}(\tilde{u}_j^{h,n}, \tilde{v}_j; \Omega_j) - (\nabla \tilde{u}_j^{h,n}, (1 - \sigma_{jk}) \nabla \tilde{v}_{I,j})_{\Omega_j} + \sum_k (\nabla \tilde{u}_j^{h,n}, \sigma_{jk} \nabla \tilde{v}_{I,j})_{\Omega_k} \\
& = (S, \tilde{v}_j)_{\Omega_j}, \quad \tilde{v}_j \in \tilde{V}_{0,j}^h, \\
\text{(b)} \quad & \sum_k (\nabla \tilde{u}_j^{h,n}, \nabla \tilde{v}_{I,j})_{\Omega_k} - i\beta \sum_k \left\langle \tilde{u}_j^{h,n}, \tilde{v}_{I,j} \right\rangle_{\Gamma_{jk}} \\
& = \sum_k (\nabla \tilde{u}_k^{h,n-1}, \nabla \tilde{v}_{I,j})_{\Omega_k} - i\beta \sum_k \left\langle \tilde{u}_k^{h,n-1}, \tilde{v}_{I,j} \right\rangle_{\Gamma_{jk}}, \quad \tilde{v}_j \in \tilde{V}_{0,j}^h,
\end{aligned} \tag{3.8}$$

where β is the relaxation parameter with $\text{Re}(\beta) > 0$. Equation (3.8b) is a matching condition on the overlapped region imposing the continuity of the discrete solution u^h on the subdomain interfaces. It can be considered as a *generalized* Robin interface boundary condition for the subproblem (3.8a). It is easy to check that each subproblem of algorithm (3.8) is well-posed for $\text{Re}(\beta) > 0$ and that the algorithm has the same solution as the original discrete problem (2.2), provided that it converges. This is an advantage of simplicity of overlapping DD methods.

We can rewrite (3.8) in the following equivalent form: given initial guess $\tilde{u}_j^{h,0} \in \tilde{V}_j^h$, $j = 1, \dots, M$, find $\tilde{u}_j^{h,n} \in \tilde{V}_j^h$, $n \geq 1$, recursively by solving

$$\begin{aligned}
& \mathcal{L}(\tilde{u}_j^{h,n}, \tilde{v}_j; \Omega_j) - (\nabla \tilde{u}_j^{h,n}, (1 - \sigma_{jk}) \nabla \tilde{v}_{I,j})_{\Omega_j} + i\beta \sum_k \left\langle \tilde{u}_j^{h,n}, \sigma_{jk} \tilde{v}_{I,j} \right\rangle_{\Gamma_{jk}} \\
& = (S, \tilde{v}_j)_{\Omega_j} - \sum_k (\nabla \tilde{u}_k^{h,n-1}, \sigma_{jk} \nabla \tilde{v}_{I,j})_{\Omega_k} + i\beta \sum_k \left\langle \tilde{u}_k^{h,n-1}, \sigma_{jk} \tilde{v}_{I,j} \right\rangle_{\Gamma_{jk}}, \quad \tilde{v}_j \in \tilde{V}_{0,j}^h.
\end{aligned} \tag{3.9}$$

It should be noticed that (3.9) can be implemented so that only the degrees of freedom on the interfaces $\cup_{j,k} \Gamma_{jk}$ are overlapped. The algorithm can be viewed as a *generalized Schwarz method* [32], where the second-order finite difference scheme was considered for solving symmetric positive definite problems.

4. CONVERGENCE ANALYSIS

In this section, we analyze algorithm (3.8) for $q(\mathbf{x}) \geq q_0 > 0$. For simplicity, assume that the mesh is uniform in a rectangular domain, having the grid size of h . Then,

$$\sigma_{jk} \equiv 1/2, \quad \text{on } \Gamma_{jk}, \quad \forall j, k. \tag{4.1}$$

Let us rewrite the terms $(\nabla \tilde{u}_j^h, \nabla \tilde{v}_{I,j})_{\Omega_j}$ and $(\nabla \tilde{u}_j^h, \nabla \tilde{v}_{I,j})_{\Omega_k}$ in (3.8), introducing operators I_{jk} and I_{kj} from $L^2(\tilde{\Omega}_j \cap \tilde{\Omega}_k)$ to $L^2(\Gamma_{jk})$ as follows:

$$\begin{aligned}
\left\langle I_{jk}(\nabla \tilde{u}_j^h), \tilde{v}_{I,j} \right\rangle_{\Gamma_{jk}} & = -(\nabla \tilde{u}_j^h, \nabla \tilde{v}_{I,j})_{\Omega_j}, \\
\left\langle I_{kj}(\nabla \tilde{u}_j^h), \tilde{v}_{I,j} \right\rangle_{\Gamma_{jk}} & = -(\nabla \tilde{u}_j^h, \nabla \tilde{v}_{I,j})_{\Omega_k}, \quad \tilde{v}_{I,j} \in \tilde{V}_{I,j}^h \cap \tilde{V}_{I,k}^h.
\end{aligned} \tag{4.2}$$

(Here we do not have to find $I_{jk}(\nabla \tilde{u}_j^h)$ and $I_{kj}(\nabla \tilde{u}_j^h)$ explicitly.) The above operators are well-defined; note that

$$(\nabla \tilde{u}_j^h, \nabla \tilde{v}_{I,j})_E = \left\langle \frac{\partial \tilde{u}_j^h}{\partial \nu_j}, \tilde{v}_{I,j} \right\rangle_{\partial E} - (\Delta \tilde{u}_j^h, \tilde{v}_{I,j})_E, \quad \tilde{v}_{I,j} \in \tilde{V}_{I,j}^h,$$

for an element $E \subset \Omega_j$ touching the interface Γ_{jk} . Since the mass-lumping quadrature rule is employed, the contribution from the nodal points not on $\partial E \cap \Gamma_{jk}$ vanishes in the integration of the right-hand terms. So

$$I_{jk}(\nabla \tilde{u}_j^h) \cong - \frac{\partial \tilde{u}_j^h}{\partial \nu_j} \Big|_{\Gamma_{jk}} + \Delta \tilde{u}_j^h \Big|_{\Gamma_{jk}} \cdot hw,$$

for some $w = w(\mathbf{x})$, $x \in \Gamma_{jk}$, which is a function of σ_{jk} and the weights of the quadrature rule. It follows from a scaling argument that

$$|I_{jk}(\nabla \tilde{u}_j^h)|_{0,\Gamma_{jk}}^2 \leq C_1 h^{-1} \|\nabla \tilde{u}_j^h\|_{0,\Omega_j \cap \tilde{\Omega}_k}^2, \quad (4.3)$$

for some $C_1 > 0$ independent of h . It is not difficult to estimate C_1 explicitly for uniform FE methods in a rectangular domain; for example, we can see $C_1 = 2$ for the bilinear FE method.

Using (3.4), (4.1), and (4.2), we rewrite (3.2) as

$$\begin{aligned} \text{(a)} \quad & \mathcal{L}(\tilde{u}_j^h, \tilde{v}_j; \Omega_j) + \sum_k \left\langle \frac{1}{2} (I_{jk}(\nabla \tilde{u}_j^h) - I_{kj}(\nabla \tilde{u}_j^h)), \tilde{v}_{I,j} \right\rangle_{\Gamma_{jk}} \\ & = (S, \tilde{v}_j)_{\Omega_j}, \quad \tilde{v}_j \in \tilde{V}_{0,j}^h, \\ \text{(b)} \quad & \tilde{u}_j^h = \tilde{u}_k^h, \quad \text{on } \tilde{\Omega}_j^h \cap \bar{\Omega}_k^h, \end{aligned} \quad (4.4)$$

and rewrite (3.8) as follows: for given initial guess $\tilde{u}_j^{h,0} \in \tilde{V}_j^h$, $j = 1, \dots, M$, find $\tilde{u}_j^{h,n} \in \tilde{V}_j^h$, $n \geq 1$, recursively by solving

$$\begin{aligned} \text{(a)} \quad & \mathcal{L}(\tilde{u}_j^{h,n}, \tilde{v}_j; \Omega_j) + \sum_k \left\langle \frac{1}{2} (I_{jk}(\nabla \tilde{u}_j^{h,n}) - I_{kj}(\nabla \tilde{u}_j^{h,n})), \tilde{v}_{I,j} \right\rangle_{\Gamma_{jk}} \\ & = (S, \tilde{v}_j)_{\Omega_j}, \quad \tilde{v}_j \in \tilde{V}_{0,j}^h, \\ \text{(b)} \quad & I_{kj}(\nabla \tilde{u}_j^{h,n}) + i\beta \tilde{u}_j^{h,n} = I_{kj}(\nabla \tilde{u}_k^{h,n-1}) + i\beta \tilde{u}_k^{h,n-1}, \quad \text{on } \Gamma_{jk}. \end{aligned} \quad (4.5)$$

Now, let

$$\tilde{e}_j^n = \tilde{u}_j^h - \tilde{u}_j^{h,n},$$

where $\{\tilde{u}_j^h\}$ is the solution of (4.4) over the partition $\{\tilde{\Omega}_j\}$ and $\{\tilde{u}_j^{h,n}\}$ are the iterates of (4.5). For the restrictions of \tilde{e}_j^n to the subspaces, we apply the same rule in (3.1).

For a simple presentation, we assume for now that $\beta = \beta_r - i\beta_i$ is a complex constant over Ω , to be determined later, and define

$$J_{r,s,t}^n = I_{rs}(\nabla \tilde{e}_t^{h,n}), \quad \text{where } r, s, t, = j, \text{ or } k, \quad \text{and } r \neq s.$$

Since the solution $\{\tilde{u}_j^h\}$ satisfies (4.5), we have

$$\begin{aligned} \text{(a)} \quad & \mathcal{L}(\tilde{e}_j^{h,n}, \tilde{v}_j; \Omega_j) + \sum_k \left\langle \frac{1}{2} (J_{jk,j}^n - J_{kj,j}^n), \tilde{v}_{I,j} \right\rangle_{\Gamma_{jk}} = 0, \quad \tilde{v}_j \in \tilde{V}_{0,j}^h, \\ \text{(b)} \quad & J_{kj,j}^n + i\beta \tilde{e}_j^{h,n} = J_{kj,k}^{n-1} + i\beta \tilde{e}_k^{h,n-1}, \quad \text{on } \Gamma_{jk}. \end{aligned} \quad (4.6)$$

Choose $\tilde{v}_j = \tilde{e}_j^n$ in (4.6a) and recall $e_j^n := \tilde{e}_j^n|_{\Omega_j}$. Then

$$\begin{aligned} & (\nabla e_j^n, \nabla e_j^n)_{\Omega_j} - ((p^2 - iq^2)e_j^n, e_j^n)_{\Omega_j} + i\langle \alpha e_j^n, e_j^n \rangle_{\Gamma_j} \\ & + \sum_k \left\langle \frac{1}{2} (J_{jk,j}^n - J_{kj,j}^n), e_j^n \right\rangle_{\Gamma_{jk}} = 0, \end{aligned} \quad (4.7)$$

so that both the real and imaginary parts of (4.7) should be zero:

$$\begin{aligned} & (\nabla e_j^n, \nabla e_j^n)_{\Omega_j} - (p^2 e_j^n, e_j^n)_{\Omega_j} + \langle \alpha_i e_j^n, e_j^n \rangle_{\Gamma_j} \\ & + \text{Re} \left(\sum_k \left\langle \frac{1}{2} (J_{jk,j}^n - J_{kj,j}^n), e_j^n \right\rangle_{\Gamma_{jk}} \right) = 0, \\ & (q^2 e_j^n, e_j^n)_{\Omega_j} + \langle \alpha_r e_j^n, e_j^n \rangle_{\Gamma_j} + \text{Im} \left(\sum_k \left\langle \frac{1}{2} (J_{jk,j}^n - J_{kj,j}^n), e_j^n \right\rangle_{\Gamma_{jk}} \right) = 0. \end{aligned} \quad (4.8)$$

Using (4.8), and with $|\cdot|_{0,\Gamma_{jk}}$ denoting the L^2 -norm on Γ_{jk} , one has

$$\begin{aligned} & \sum_k |J_{kj,j}^n + i\beta e_j^n|_{0,\Gamma_{jk}}^2 \\ & = \sum_k \{ |J_{kj,j}^n|_{0,\Gamma_{jk}}^2 + |\beta|^2 |e_j^n|_{0,\Gamma_{jk}}^2 \} \\ & \quad + 2\beta_r \text{Im} \left(\sum_k \langle J_{kj,j}^n, e_j^n \rangle_{\Gamma_{jk}} \right) + 2\beta_i \text{Re} \left(\sum_k \langle J_{kj,j}^n, e_j^n \rangle_{\Gamma_{jk}} \right) \\ & = \sum_k \{ |J_{kj,j}^n|_{0,\Gamma_{jk}}^2 + |\beta|^2 |e_j^n|_{0,\Gamma_{jk}}^2 \} + 4\beta_r \{ (q^2 e_j^n, e_j^n)_{\Omega_j} + \langle \alpha_r e_j^n, e_j^n \rangle_{\Gamma_j} \} \\ & \quad + 4\beta_i \{ (\nabla e_j^n, \nabla e_j^n)_{\Omega_j} - (p^2 e_j^n, e_j^n)_{\Omega_j} + \langle \alpha_i e_j^n, e_j^n \rangle_{\Gamma_j} \} \\ & \quad + 2\beta_r \text{Im} \left(\sum_k \langle J_{jk,j}^n, e_j^n \rangle_{\Gamma_{jk}} \right) + 2\beta_i \text{Re} \left(\sum_k \langle J_{jk,j}^n, e_j^n \rangle_{\Gamma_{jk}} \right), \end{aligned} \quad (4.9)$$

$$\begin{aligned} & \sum_k |J_{jk,j}^n + i\beta e_j^n|_{0,\Gamma_{jk}}^2 \\ & = \sum_k \{ |J_{jk,j}^n|_{0,\Gamma_{jk}}^2 + |\beta|^2 |e_j^n|_{0,\Gamma_{jk}}^2 \} \\ & \quad + 2\beta_r \text{Im} \left(\sum_k \langle J_{jk,j}^n, e_j^n \rangle_{\Gamma_{jk}} \right) + 2\beta_i \text{Re} \left(\sum_k \langle J_{jk,j}^n, e_j^n \rangle_{\Gamma_{jk}} \right). \end{aligned} \quad (4.10)$$

Set

$$E(e) = \sum_j \sum_k |J_{kj,j} + i\beta e_j|_{0,\Gamma_{jk}}^2, \quad (4.11)$$

and let $E^n = E(e^n)$. Then, from (4.6b) and (4.9)-(4.10),

$$\begin{aligned} E^n &= \sum_j \sum_k |J_{kj,j}^n + i\beta e_j^n|_{0,\Gamma_{jk}}^2 = \sum_j \sum_k |J_{kj,k}^{n-1} + i\beta e_k^{n-1}|_{0,\Gamma_{jk}}^2 \\ &= E^{n-1} - R^{n-1}, \end{aligned} \quad (4.12)$$

where

$$\begin{aligned} R^n &:= R(e^n) \\ &= \sum_j \sum_k |J_{kj,j}^n|_{0,\Gamma_{jk}}^2 - \sum_j \sum_k |J_{kj,k}^n|_{0,\Gamma_{jk}}^2 \\ &\quad + 4\beta_r \sum_j \{(q^2 e_j^n, e_j^n)_{\Omega_j} + \langle \alpha_r e_j^n, e_j^n \rangle_{\Gamma_j}\} \\ &\quad + 4\beta_i \sum_j \{(\nabla e_j^n, \nabla e_j^n)_{\Omega_j} - (p^2 e_j^n, e_j^n)_{\Omega_j} + \langle \alpha_i e_j^n, e_j^n \rangle_{\Gamma_j}\}. \end{aligned}$$

We will choose $\beta = \beta_r - i\beta_i$ such that R^n , $n \geq 0$, are nonnegative. Recall (4.3):

$$\sum_j \sum_k |J_{kj,k}^n|_{0,\Gamma_{jk}}^2 \leq C_1 h^{-1} \sum_j \sum_k \|\nabla e_j^{h,n}\|_{0,\Omega_j \cap \tilde{\Omega}_k}^2,$$

and notice

$$(p^2 e_j^n, e_j^n)_{\Omega_j} \leq \frac{p_1^2}{q_0^2} (q^2 e_j^n, e_j^n)_{\Omega_j}.$$

Let

$$\beta_i \geq \frac{C_1 h^{-1}}{4} \quad \text{and} \quad \beta_r \geq \beta_i \frac{p_1^2}{q_0^2}. \quad (4.13)$$

Then, for $j = 1, \dots, M$,

$$\begin{aligned} \text{(a)} \quad \sum_k |J_{kj,k}^n|_{0,\Gamma_{jk}}^2 &\leq 4\beta_i \sum_k (\nabla e_j^n, \nabla e_j^n)_{\Omega_j \cap \tilde{\Omega}_k}, \\ \text{(b)} \quad 4\beta_i (p^2 e_j^n, e_j^n)_{\Omega_j} &\leq 4\beta_r (q^2 e_j^n, e_j^n)_{\Omega_j}. \end{aligned} \quad (4.14)$$

The inequalities in (4.14) imply that $R^n \geq 0$, $n \geq 0$, i.e., $\{E^n\}$ is a decreasing sequence of nonnegative numbers. So, from (4.12), we have

$$\sum_{n=0}^{\infty} R^n = \lim_{k \rightarrow \infty} \sum_{n=0}^k (E^n - E^{n+1}) = E^0 - \lim_{k \rightarrow \infty} E^{k+1} \leq E^0 < \infty,$$

which implies $\lim_{n \rightarrow \infty} R^n \searrow 0$. Since R^n has two negative terms, the choice of β in (4.13) may not guarantee $e^n \rightarrow 0$, unless at least one of the inequalities in (4.13) is strict; choose $\beta = \beta_r - i\beta_i$ such that

$$\frac{C_1 h^{-1}}{4} \leq \beta_i < \beta_r \frac{q_0^2}{p_1^2}. \quad (4.15)$$

Then, for each $n \geq 0$, we have

$$R^n \geq 4\beta_r \sum_j (q^2 e_j^n, e_j^n)_{\Omega_j} - 4\beta_i \sum_j (p^2 e_j^n, e_j^n)_{\Omega_j} \geq 4\delta \sum_j (e_j^n, e_j^n)_{\Omega_j}, \quad (4.16)$$

where

$$\delta = \beta_r q_0^2 - \beta_i p_1^2 > 0.$$

Note that $R^n \rightarrow 0$ as $n \rightarrow \infty$. So

$$e_j^n \rightarrow 0 \text{ in } L^2(\Omega_j), \quad j = 1, \dots, M, \text{ as } n \rightarrow \infty.$$

We have proved the convergence of algorithm (3.8) as stated in the following theorem.

Theorem 4.1. *Assume $q(\mathbf{x}) \geq q_0 > 0$ and let $\beta = \beta_r - i\beta_i$ be given as in (4.15). Then the iterates $\{\tilde{u}_j^{h,n}\}$ of algorithm (3.8) converge to the solution $\{\tilde{u}_j^h\}$ of (3.2) in the following sense:*

$$\tilde{u}_j^{h,n}|_{\Omega_j} \rightarrow \tilde{u}_j^h|_{\Omega_j} = u^{h,*}|_{\Omega_j} \text{ in } L^2(\Omega_j), \quad j = 1, \dots, M,$$

where $u^{h,*} \in V^h$ is the original discrete solution of (2.2).

Now, let \mathcal{B} be an affine mapping from V^h to itself such that, for any $\theta \in V^h$, $e := \mathcal{B}(\theta)$ is the solution for the following equation:

$$\begin{aligned} \mathcal{L}(\tilde{e}_j, \tilde{v}_j; \Omega_j) + \sum_k \left\langle \frac{1}{2} (I_{jk}(\nabla e_j) + i\beta e_j), \tilde{v}_{I,j} \right\rangle_{\Gamma_{jk}} \\ = \sum_k \left\langle \frac{1}{2} (I_{kj}(\nabla \theta_k) + i\beta \theta_k), \tilde{v}_{I,j} \right\rangle_{\Gamma_{jk}}, \quad \tilde{v}_j \in \tilde{V}_{0,j}^h. \end{aligned} \quad (4.17)$$

Theorem 4.2. *Assume $q(\mathbf{x}) \geq q_0 > 0$. Let $\beta = \beta_r - i\beta_i$ be given as in (4.15) and $\rho(\mathcal{B})$ be the spectral radius of \mathcal{B} . Then*

$$\rho(\mathcal{B}) < 1. \quad (4.18)$$

Proof. Let $\{\gamma, e\}$ be an eigenvalue-eigenvector pair of \mathcal{B} ; i.e., $\mathcal{B}(e) = \gamma e$. Our objective is to show that $|\gamma| < 1$. It follows from (4.11)-(4.12) that

$$\begin{aligned} E(\mathcal{B}(e)) &= |\gamma|^2 E(e), \\ E(\mathcal{B}(e)) &= E(e) - R(e). \end{aligned}$$

Combining the two equations above yields

$$|\gamma|^2 = (E(e) - R(e)) / E(e), \quad (4.19)$$

which implies that $|\gamma| \leq 1$. Equality holds if and only if $R(e) = 0$, so that from (4.16) we have $e \equiv 0$. This contradicts the fact that the eigenvectors are non-trivial, which completes the proof. \square

Now, we will check the asymptotic rate of convergence for (3.8). For convenience, we choose $\beta = \beta_r - i\beta_i$ as

$$\beta_i = \frac{C_1 h^{-1}}{4}, \quad \beta_r = \xi \beta_i \frac{p_1^2}{q_0^2}, \quad \xi > 1. \quad (4.20)$$

Then

$$|\beta|^2 \leq S\beta_r^2, \quad \text{where } S = 1 + \frac{q_0^4}{p_1^4}. \quad (4.21)$$

Let

$$\begin{aligned} E_j(e) &= \sum_k |J_{kj,j} + i\beta e_j|_{0,\Gamma_{jk}}^2, \\ R_j(e) &= \sum_k |J_{kj,j}|_{0,\Gamma_{jk}}^2 - \sum_k |J_{kj,k}|_{0,\Gamma_{jk}}^2 \\ &\quad + 4\beta_r \{ (q^2 e_j, e_j)_{\Omega_j} + \langle \alpha_r e_j, e_j \rangle_{\Gamma_j} \} \\ &\quad + 4\beta_i \{ (\nabla e_j, \nabla e_j)_{\Omega_j} - (p^2 e_j, e_j)_{\Omega_j} + \langle \alpha_i e_j, e_j \rangle_{\Gamma_j} \}, \\ R'_j(e) &= \sum_k |J_{kj,j}|_{0,\Gamma_{jk}}^2 + 4\beta_r (q^2 e_j, e_j)_{\Omega_j}. \end{aligned}$$

Lemma 4.3. *Let β be chosen as in (4.20). Then*

$$R'_j(e) \leq \frac{\xi}{\xi - 1} R_j(e), \quad j = 1, 2, \dots, M. \quad (4.22)$$

Proof. Note that

$$(\xi - 1) \frac{p_1^2}{q_0^2} (q^2 e_j, e_j)_{\Omega_j} \leq \xi \frac{p_1^2}{q_0^2} (q^2 e_j, e_j)_{\Omega_j} - (p^2 e_j, e_j)_{\Omega_j}.$$

Multiplying both sides of the above inequality by $4\beta_i \xi / (\xi - 1)$ and using (4.20), we have

$$4\beta_r (q^2 e_j, e_j)_{\Omega_j} \leq \frac{\xi}{\xi - 1} \{ 4\beta_r (q^2 e_j, e_j)_{\Omega_j} - 4\beta_i (p^2 e_j, e_j)_{\Omega_j} \}. \quad (4.23)$$

From (4.14a),

$$\begin{aligned} \sum_k |J_{kj,j}|_{0,\Gamma_{jk}}^2 &\leq \sum_k |J_{kj,j}|_{0,\Gamma_{jk}}^2 - \sum_k |J_{kj,k}|_{0,\Gamma_{jk}}^2 + 4\beta_i (\nabla e_j, \nabla e_j)_{\Omega_j} \\ &\leq \frac{\xi}{\xi - 1} \left\{ \sum_k |J_{kj,j}|_{0,\Gamma_{jk}}^2 - \sum_k |J_{kj,k}|_{0,\Gamma_{jk}}^2 + 4\beta_i (\nabla e_j, \nabla e_j)_{\Omega_j} \right\}. \end{aligned}$$

Then, (4.22) follows from the above and (4.23). \square

There is a positive constant K_1 , independent of h , such that

$$\sum_k |u_j|_{0,\Gamma_{jk}}^2 \leq K_1 h^{-1} \|u_j\|_{0,\Omega_j}^2, \quad \forall u_j \in V_j^h, \quad j = 1, 2, \dots, M. \quad (4.24)$$

From the Schwarz inequality and (4.21)-(4.24), we have

$$\begin{aligned} E_j(e) &\leq 2 \sum_k |J_{kj,j}|_{0,\Gamma_{jk}}^2 + 2|\beta|^2 \sum_k |e_j|_{0,\Gamma_{jk}}^2 \\ &\leq 2 \sum_k |J_{kj,j}|_{0,\Gamma_{jk}}^2 + 2S\beta_r^2 K_1 h^{-1} \|e_j\|_{0,\Omega_j}^2 \\ &\leq \left(2 + SK_1 h^{-1} \frac{\beta_r}{2q_0^2}\right) R_j'(e) \\ &\leq g(\xi) R_j(e), \end{aligned} \quad (4.25)$$

where

$$g(\xi) = \frac{\xi}{\xi - 1} \left(2 + SC_1 K_1 p_1^2 h^{-2} \frac{\xi}{8q_0^4}\right).$$

So, from (4.19) and (4.25),

$$|\gamma|^2 \leq 1 - \frac{1}{g(\xi)},$$

and therefore

$$|\gamma| \leq 1 - \frac{1}{2g(\xi)}. \quad (4.26)$$

It is not difficult to check that $g(\xi)$ can be minimized when

$$\xi = 1 + \left(1 + \frac{16h^2 q_0^4}{SC_1 K_1 p_1^2}\right)^{1/2}. \quad (4.27)$$

After substituting (4.27) into (4.26), one can get the following result.

Theorem 4.4. *Let the relaxation parameter $\beta = \beta_r - i\beta_i$ for algorithm (3.8) be chosen as in (4.20) and (4.27). Then the spectral radius of the iteration matrix of algorithm (3.8) is minimized and bounded as*

$$\rho(\mathcal{B}) \leq 1 - C_2 \frac{q_0^4}{p_1^2} h^2, \quad (4.28)$$

for some $C_2 > 0$ independent of h , p , and q .

Now, let us consider a real-valued relaxation parameter. Let

$$\beta = \beta_r > \frac{C_3}{q_0^2} h^{-3}, \quad (4.29)$$

for some $C_3 > 0$. (For FE methods of uniform meshes, $C_3 = 4$.) Then it is not difficult to prove the convergence of (3.8). Furthermore, using the above arguments, one can conclude an analogue of Theorem 4.4: Choose

$$\beta = \beta_r = \xi \frac{C_3}{q_0^2} h^{-3}, \quad \xi = 1 + \left(1 + \frac{4q_0^4 h^4}{C_3 K_1}\right)^{1/2}. \quad (4.30)$$

Then, the spectral radius of the iteration matrix of (3.8) is minimized and bounded as

$$\rho(\mathcal{B}) \leq 1 - C_4 q_0^4 h^4, \quad (4.31)$$

for some $C_4 > 0$ independent of h , p , and q .

For general cases, i.e., $q \geq q_0 \geq 0$, we do not know of any convergence analysis for (3.8). As mentioned in Section 2, the positivity of q_0 is the same as the existence of a convergent nonsymmetric CG-type algorithm [17, 18].

The right-hand side of (4.28) is most sensitive to the attenuation coefficient q . When q increases (a little, though), the convergence would be significantly improved. This is the motivation of the artificial damping technique introduced in the next section.

5. ARTIFICIAL DAMPING ITERATION

For the propagation of waves in slightly- or non-attenuate media, it is well known that most iterative algorithms either converge slowly or fail to converge, as mentioned earlier. For these cases, we can apply so called the *artificial damping iteration* (ArtDI) which was first proposed in [24] and refined in [21]. For a completeness of the paper we will present the idea of ArtDI. We first consider the following lemma.

Lemma 5.1. [21] *Let λ be an eigenvalue of A . Then $\text{Im}(\lambda) \geq 0$.*

For the ArtDI, choose $\eta > 0$ and an initial guess $u^{h,0} \in V^h$. Then we find $u^{h,\ell} \in V^h$, $\ell \geq 1$, by recursively solving

$$\mathcal{L}(u^{h,\ell}, v; \Omega) + (i\eta^2 u^{h,\ell}, v)_\Omega = (S, v)_\Omega + (i\eta^2 u^{h,\ell-1}, v)_\Omega, \quad \forall v \in V^h. \quad (5.1)$$

Using notations in (2.4), we can rewrite (5.1) in a matrix form as

$$(A + iD) \mathbf{u}^{h,\ell} = \mathbf{b} + iD \mathbf{u}^{h,\ell-1}. \quad (5.2)$$

Recall we use a mass-lumping quadrature rule; matrix D is diagonal with positive entries. We may choose $\eta(\mathbf{x})$ such that $D = \text{diag}\{d\}$, for some constant $d > 0$. Let \mathbf{u}^h be the solution vector of (2.4) and $\mathbf{e}^\ell = \mathbf{u}^h - \mathbf{u}^{h,\ell}$. Then, it follows from (2.4) and (5.2) that

$$(A + idI) \mathbf{e}^\ell = id \mathbf{e}^{\ell-1}, \quad (5.3)$$

and therefore

$$\|\mathbf{e}^\ell\| \leq \max_{\lambda \in \sigma(A)} \left| \frac{id}{\lambda + id} \right| \cdot \|\mathbf{e}^{\ell-1}\|.$$

It follows from Lemma 5.1 that (5.1) converges for all $d > 0$ unless $0 \in \sigma(A)$.

It seems each step of (5.1) is the same (in problem size) as the original problem, but it has the new wave number \widehat{K} given as

$$\widehat{K}^2 = K^2 - i\eta^2 = p^2 - i(q^2 + \eta^2) =: \widehat{K}_r^2 - i\widehat{K}_i^2.$$

Note that the right-hand side of (4.28) is very sensitive to \widehat{K}_i^2 which is larger than q^2 . Hence we can solve each step of algorithm (5.1), a damped problem, much more efficiently by employing algorithm (3.8) as the inner loop. As usual, the inner loop can be solved *incompletely* by either loosening the stopping criterion or choosing an upper limit on the iteration count. The following was proposed in [21]: select $\eta > 0$, $n_* > 0$, and an initial guess $\tilde{u}_j^{h,0} = u^{h,0}|_{\tilde{\Omega}_j}$, $j = 1, \dots, M$, and find $\tilde{u}_j^{h,\ell,n}$, $\ell \geq 1$, $1 \leq n \leq n_*$ (for each fixed ℓ), by solving

$$\begin{aligned} \text{(a)} \quad & \mathcal{L}(\tilde{u}_j^{h,\ell,n}, \tilde{v}_j; \Omega_j) + (i\eta^2 \tilde{u}_j^{h,\ell,n}, \tilde{v}_j)_{\Omega_j} - (\nabla \tilde{u}_j^{h,\ell,n}, (1 - \sigma_{jk}) \nabla \tilde{v}_{I,j})_{\Omega_j} \\ & + \sum_k (\nabla \tilde{u}_j^{h,\ell,n}, \sigma_{jk} \nabla \tilde{v}_{I,j})_{\Omega_k} = (S, \tilde{v}_j)_{\Omega_j} + (i\eta^2 \tilde{u}_j^{h,\ell,0}, \tilde{v}_j)_{\Omega_j}, \quad \tilde{v}_j \in \tilde{V}_{0,j}^h, \\ \text{(b)} \quad & \sum_k (\nabla \tilde{u}_j^{h,\ell,n}, \nabla \tilde{v}_{I,j})_{\Omega_k} - i\beta \sum_k \langle \tilde{u}_j^{h,\ell,n}, \tilde{v}_{I,j} \rangle_{\Gamma_{jk}} \\ & = \sum_k (\nabla \tilde{u}_k^{h,\ell,n-1}, \nabla \tilde{v}_{I,j})_{\Omega_k} - i\beta \sum_k \langle \tilde{u}_k^{h,\ell,n-1}, \tilde{v}_{I,j} \rangle_{\Gamma_{jk}}, \quad \tilde{v}_j \in \tilde{V}_{0,j}^h, \\ \text{(c)} \quad & \tilde{u}_j^{h,\ell,0} = \begin{cases} \tilde{u}_j^{h,0}, & \text{if } \ell = 1, \\ \tilde{u}_j^{h,\ell-1,n_*}, & \text{if } \ell \neq 1. \end{cases} \end{aligned} \tag{5.4}$$

For n_* sufficiently large, one can show the convergence of algorithm (5.4) even for the non-attenuate wave propagation ($q \equiv 0$). However, we are more interested in the problem of choosing parameters, η and n_* , in a computationally efficient manner. Note that when $(\eta, n_*) = (0, 1)$, the algorithm (5.4) turns out to be (3.8).

6. NUMERICAL RESULTS

In this section, we verify accuracy and efficiency of algorithms (3.8) and (5.4) for solving the Helmholtz equation in 2D media by FE methods, for various choices of h , r , η , and n_* . Set the domain $\Omega = (0, 1)^2$; we consider uniform quadrilateral elements of the edge length $h = 1/n_p$, for $n_p > 0$, and the finite element methods incorporating Legendre-Gauss-Lobatto splines of order r . The algorithm is implemented in C++ for the main function and FORTRAN for the others and carried out on a 16-node cluster of 2.4 Ghz Pentium 4 processors, with 512MB RAM memory for each. The wave number is selected as

$$p(\mathbf{x}) = \omega/v(\mathbf{x}),$$

where ω ($:= 2\pi f$) denotes the angular frequency. Here f is the frequency. The wave speed $v(\mathbf{x})$ is chosen as follows:

$$\begin{aligned} v_1(x, y) &\equiv 1, \\ v_2(x, y) &= 1.6 + |\sin 3\pi x \cos 4\pi y|, \\ v_3(x, y) &= \begin{cases} 2, & \text{if } (x, y) \in [0.45, 0.75] \times [0.55, 0.75], \\ 1, & \text{otherwise.} \end{cases} \end{aligned}$$

Note that v_2 is continuous (but not smooth) and v_3 is piecewise constant. For the ABC, we set $\alpha(\mathbf{x}) = p(\mathbf{x})$.

Since we are interested in the propagation of waves in slightly- or non-attenuate media, the quality factor can be defined by

$$Q := \frac{p^2}{q^2} = \frac{\omega^2}{v^2 q^2} \in (0, \infty], \quad (6.1)$$

where $Q = \infty$ for $q = 0$. The quality factor is known to be between 50 and 300 in most earth media. The higher it is, the less attenuate and therefore the harder to solve (1.1). The quality factor has the following physical interpretation: after traveling Q wavelengths, waves are reduced in magnitude by a factor of $e^{-\pi}$, compared with non-attenuate waves [3]. The wavelength is by definition v/f ($= 2\pi v/\omega = 2\pi/p$). In this article the attenuation coefficient $q(\mathbf{x})$ will be determined from values of Q , ω , and $v(\mathbf{x})$ and utilizing (6.1).

Let $S_t(\mathbf{x})$ be the source that corresponds to the following true solution

$$u(\mathbf{x}) = \frac{\phi(x) \cdot \phi(y)}{\omega^2}, \quad (6.2)$$

where $\phi(x) = e^{i\omega(x-1)} + e^{-i\omega x} - 2$, and $S_{\mathbf{x}_0}(\mathbf{x}) = \delta(\mathbf{x} - \mathbf{x}_0)$, for some $\mathbf{x}_0 \in \bar{\Omega}$.

One can decompose the domain in various ways. However, for simplicity, we consider the element-wise decomposition; for parallelism, strips of subdomains are equally divided and assigned to the processors. The wall-clock time is denoted by CPU (in seconds) and the iteration is stopped when the iterates satisfy the following stopping criterion

$$\frac{\|u^{h,m} - u^{h,m-1}\|_\infty}{\|u^{h,m}\|_\infty} < \mathbf{tol},$$

where \mathbf{tol} is the tolerance, m is n or ℓ which is the iteration index respectively for (3.8) or (5.4). The tolerance will be chosen as $\mathbf{tol} = 10^{-\gamma}$, $\gamma = 4, 8, \text{ or } 12$, depending on the solution accuracy. Zero initial values are given: $u^{h,0} \equiv 0$, for all examples dealt in this article. The total number of DD iterations is denoted by N and therefore $N = m$ for (3.8) and $N = m \cdot n_*$ for (5.4). For $S = S_t$, the numerical error is measured by the relative L^2 norm

$$r_0^N = \frac{\|u^{h,N} - u\|_0}{\|u\|_0},$$

Table 1: Effectiveness of ArtDI. Set $S = S_t$, $v = v_1$, $Q = \infty$, and $\text{tol} = 1.0\text{e-}04$.

$1/h = 160, r = 1, f = 5$					$1/h = 320, r = 2, f = 30$				
η	n_*	N	CPU	r_0^N	η	n_*	N	CPU	r_0^N
0	1	880	1.9	1.91e-02	0	1			diverges
10	10	770	1.3	1.90e-02	30	25			diverges
10	20	520	0.8	1.90e-02	50	25	925	23.5	3.02e-03
20	20	800	1.5	1.90e-02	50	50	1100	26.8	3.20e-03

where u is the true solution in (6.2).

Regarding the choice of the relaxation parameter β on the subdomain interfaces, we have employed the *alternating direction optimal procedure* (ADOP) [21] in a modified form. ADOP seeks $\beta = \beta(\mathbf{x})$ in such a way that the spectral radii of the iteration matrices of the one-dimensional reduction problems are all zero; see Kim [21] for details. It should be noticed that ADOP is automatic and computationally inexpensive.

In table 1, we first verify effectiveness of the ArtDI. We have tested the algorithm for various choices of η and n_* . As one can see from the table, the choice of (η, n_*) is important for the simulation of non-attenuate waves ($Q = \infty$). Note that the ArtDI method (5.4) with the choice $(\eta, n_*) = (0, 1)$ becomes the DD algorithm (3.8). As shown in the convergence analysis, the DD algorithm (without ArtDI) fails to converge for most of high-frequency solutions in non-attenuate media. The iteration count n_* must be set large enough to incorporate the ArtDI appropriately and effectively. It has been numerically verified that n_* can be selected solely depending on the grid size h , while the selection of η is more complicated due to its dependence on h and the wave number (ω/v) as well. However, a good thing is that the quality factor Q and the degree of basis functions r have shown little effect on the selection of the parameters η and n_* .

For all examples in the remainder of the section, we will choose n_* and η as follows:

$$\begin{aligned} n_* &= n_p/\kappa, \quad \kappa = 8 \sim 16, \\ \eta^2 &= \bar{p}^2/Q_a, \quad Q_a = 10 \sim 20, \end{aligned} \tag{6.3}$$

where \bar{p} denotes the L^2 -average of $p = \omega/v$ over the domain and Q_a is the artificial quality factor. We set κ larger as n_p increases (i.e., n_* grows with n_p sublinearly) and select Q_a smaller as \bar{p} or h increases.

Table 2 shows convergence rates of numerical error (with respect to the grid size h) for various spline orders r , carried out by utilizing the algorithm (5.4). We choose $f = 5$, $S = S_t$, $v = v_1$, $Q = \infty$, and $\text{tol} = 1.0\text{e-}12$. Note that the tolerance is chosen to be small ($1.0\text{e-}12$) so as to incorporate higher accuracy of higher-order FE methods. In view of (2.3), the convergence rate is as expected for $r = 1$ (the 2nd-order FE

Table 2: Convergence rates of the error with respect to the grid size h , for various orders of shape functions r . Set $f = 5$, $S = S_t$, $v = v_1$, $Q = \infty$, and $\text{tol} = 1.0\text{e-}12$. Superconvergence occurs for $r \geq 2$.

$r = 1$					$r = 2$				
$1/h$	N	CPU	r_0^N	rate	$1/h$	N	CPU	r_0^N	rate
64	741	0.2	1.13e-01		64	703	0.5	2.31e-04	
128	1540	2.4	2.81e-02	2.00	128	1340	5.6	1.43e-05	4.01
256	3696	16.8	7.00e-03	2.00	256	3674	63.7	8.94e-07	4.00
$r = 3$					$r = 4$				
$1/h$	N	CPU	r_0^N	rate	$1/h$	N	CPU	r_0^N	rate
64	684	2.6	1.10e-06		48	646	3.0	7.69e-08	
128	1580	24.8	3.33e-08	5.04	96	1140	21.3	1.19e-09	6.01
256	4334	281.5	1.03e-09	5.01	192	3420	273.7	1.86e-11	6.00

Table 3: Destruction rates of FE solutions with respect to the frequency f , for various orders of shape functions r . Set $S = S_t$, $v = v_1$, and $Q = 100$.

$r = 1$ ($1/h = 640$, $\text{tol} = 1.0\text{e-}08$)					$r = 2$ ($1/h = 320$, $\text{tol} = 1.0\text{e-}08$)				
f	N	CPU	r_0^N	rate	f	N	CPU	r_0^N	rate
8	5720	164.8	4.82e-03		8	3666	92.2	3.96e-06	
16	4000	114.6	3.87e-02	3.00	16	3042	76.9	1.27e-04	5.00
32	8440	239.7	3.09e-01	3.00	32	3224	81.1	4.14e-03	5.03
$r = 3$ ($1/h = 320$, $\text{tol} = 1.0\text{e-}12$)					$r = 4$ ($1/h = 192$, $\text{tol} = 1.0\text{e-}12$)				
f	N	CPU	r_0^N	rate	f	N	CPU	r_0^N	rate
5	5876	533.5	3.38e-10		5	3255	226.9	1.87e-11	
10	2912	265.6	1.10e-08	5.02	10	1617	113.4	1.19e-09	5.99
20	2178	123.3	4.17e-07	5.24	20	1638	114.1	7.71e-08	6.02

method); however, the remaining cases ($r \geq 2$) in the table show that the actual convergence rate is one order higher than expected. We do not know the reason for such a superconvergence phenomenon. A detailed analysis is needed to clarify it.

In Table 3, we present the destruction rates of FE solutions with respect to the frequency, for various orders of shape functions r . We choose $S = S_t$, $v = v_1$, and $Q = 100$. As one can see from the table, the results match with the theoretical expectation in (2.3) except for $r = 2$. When $r = 2$, the actual destruction rate of the solution with respect to the frequency is one order higher than expected. Again the reason for such a phenomenon is not clear for us at this moment; FE methods need to be analyzed in detail to clarify it.

Table 4 shows the performance of the ArtDI (5.4) for various spline orders r . Set

Table 4: Accuracy-efficiency test. Set $S = S_t$, $Q = \infty$, and $\text{tol} = 1.0e - 08$.

$f = 10$		$v = v_1$			$v = v_2$			$v = v_3$		
$1/h$	r	N	CPU	r_0^N	N	CPU	r_0^N	N	CPU	r_0^N
384	1	2842	28.8	2.59e-02	3219	32.6	2.88e-03	6815	69.3	2.44e-02
192	2	1140	10.0	9.22e-05	1580	13.8	1.56e-05	1320	11.6	8.65e-05
128	3	840	11.7	1.19e-06	1060	14.7	1.06e-06	6180	85.2	1.18e-06
96	4	720	12.2	7.76e-08	920	15.7	7.71e-08	9860	167.3	8.55e-08
$f = 30$		$v = v_1$			$v = v_2$			$v = v_3$		
$1/h$	r	N	CPU	r_0^N	N	CPU	r_0^N	N	CPU	r_0^N
768	1	6390	263.8	1.72e-01	4410	182.2	7.21e-03	9135	376.7	1.62e-01
384	2	2117	77.9	1.39e-03	2088	77.2	7.71e-05	3393	125.4	1.31e-03
256	3	1606	91.3	1.98e-05	1430	81.9	8.11e-06	11572	659.1	1.89e-05
192	4	1380	97.3	9.31e-07	1280	90.1	8.70e-07	12240	860.6	9.30e-07

$S = S_t$, $Q = \infty$, and $\text{tol} = 1.0e-08$ for all the results. Note that r/h is set to be the same as 384 for the first part ($f = 10$) and 768 for the second part ($f = 30$), which implies that the number of grid points is the same in each part. As one can see from the table, the case $r = 2$ gives the smallest CPU time, while higher-order ones ($r \geq 3$) produce more accurate results. When the velocity is continuous ($v = v_1$ and $v = v_2$), the higher-order FE methods ($r \geq 3$) turn out to be slightly more expensive computationally, while they improve accuracy a lot. One can easily expect that higher-order FE methods ($r \geq 3$) may result in a more efficient method for a fixed accuracy, when the medium is smooth enough. On the other hand, for the discontinuous velocity ($v = v_3$), the higher-order methods cost much more for a relatively small accuracy improvement over the case that $r = 2$. We recommend to employ the FE method of quadratic splines for the simulation of waves in discontinuous media.

We will close the section showing a high-frequency numerical solution in $v = v_3$ for a point source.

In Figure 3, we depict the real part of a numerical solution which is obtained with parameters: $1/h = 320$, $f = 50$, $v = v_3$, $Q = \infty$, $S = \delta(\mathbf{x} - \mathbf{x}_0)$, $\mathbf{x}_0 = (0.25, 0.20)$, $r = 2$, and $\text{tol} = 1.0e-08$. The ArtDI is set up with $\eta = 100$ and $n_* = 25$. Lighter parts indicate higher values in the picture; a gain function of the form $1 + |\mathbf{x} - \mathbf{x}_0|$ has been multiplied for a better look of the numerical solution, in particular, in regions far away from the source. The ArtDI converges in 1325 DD iterations (53 outer iterations), taking 32.5s of wall-clock time for 16 nodes. It is clear to see from the figure that the velocity discontinuity has introduced reflection and refraction (the change in direction of wave rays upon passing into a medium with different velocity). It should be noticed that no apparent phase lag has been observed; the expected

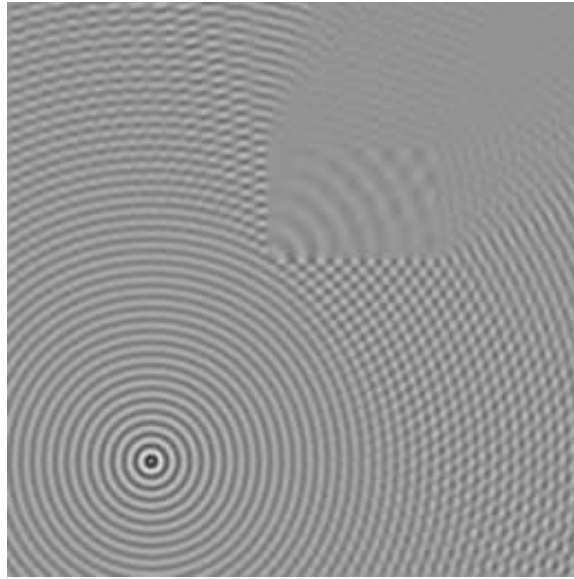


Figure 3: The real part of a high-frequency numerical solution. Set $1/h = 320$, $f = 50$, $v = v_3$, $Q = \infty$, $S = S_{\mathbf{x}_0}$, $\mathbf{x}_0 = (0.25, 0.20)$, $r = 2$, and $\text{tol} = 1.0\text{e-}08$. Lighter parts indicate higher values. Reflection and refraction have been observed through the velocity discontinuity.

number of wavelengths is 50 on the vertical line passing the source, as counted there. For this example, the number of grid points per wavelength ($:= rv/(fh)$) is 12.8 for the region where $v = 1$.

7. CONCLUSIONS

A domain decomposition (DD) iterative procedure for solving the Helmholtz wave problem by finite element (FE) methods has been considered. We have chosen minimum-overlapping subdomains and employed a Robin interface boundary condition in a modified form. Under certain assumptions on the mesh and the quadrature rule, we could prove the convergence of the algorithm for attenuate waves. For slightly- or non-attenuate waves, we have introduced the artificial damping iteration (ArtDI) as an outer iteration of the DD method, the convergence of which can be proved when the inner iteration is solved accurately enough. The resulting algorithm combining the ArtDI and DD iterations has been tested for the numerical solution of the Helmholtz problem in 2D media for various spline orders r and diverse frequencies f . For high-order FE methods ($r \geq 2$), the numerical error (with respect to the grid size) has converged one-order higher than expected from the theory of numerical accuracy. As the frequency increases, the numerical accuracy has been destructed as expected except for $r = 2$. A detailed analysis is required to figure out why a destruction of one-order higher has occurred for the FE method of quadratic splines. However, for the element-wise domain decomposition, the FE method of

quadratic splines is recommended for the simulation of waves in discontinuous media; higher-order methods introduce little improvement in the accuracy of the numerical solution in discontinuous media. When the medium is smooth enough, higher-order FE methods have proved more efficient for a fixed accuracy.

The algorithm presented in this paper can be applied to solving vector waves such as electromagnetic waves and viscoelasticity in the frequency domain [6]. It is expected to be similarly accurate and efficient as in the scalar waves, provided that one can determine the parameters (β , η , and n_*) effectively.

REFERENCES

- [1] A. BAYLISS, C. GOLDSTEIN, AND E. TURKEL, *An iterative method for the Helmholtz equation*, J. Comput. Phys., 49 (1983), pp. 443–457.
- [2] ———, *On accuracy conditions for the numerical computation of waves*, J. Comput. Phys., 59 (1985), pp. 396–404.
- [3] T. BOURBIE, O. COUSSY, AND B. ZINSZNER, *Acoustics of porous media*, Institut francais du petrole publications, Gulf Publishing Company, Houston, London, Paris, Tokyo, 1987. Translated from the French by Nissim Marshall.
- [4] X.-C. CAI, M. CASARIN, F. ELLIOTT, JR., AND O. WIDLUND, *Overlapping Schwarz algorithms for solving Helmholtz's equation*, in Domain Decomposition Methods 10, J. Mandel, C. Farhat, and X.-C. Cai, eds., vol. 218 of Contemporary Mathematics, Providence, RI, 1998, American Mathematical Society, pp. 391–399. Proceedings of the Tenth International Conference on Domain Decomposition Methods, August 10-14, 1997, Boulder, CO.
- [5] C. CANUTO, M. Y. HUSSAINI, A. QUARTERONI, AND T. A. ZANG, *Spectral methods in fluid dynamics*, Springer Verlag, 1987.
- [6] Y. CHA AND S. KIM, *Domain decomposition methods for the linear viscoelasticity*. (in preparation).
- [7] P. CIARLET, *The Finite Element Method for Elliptic Equations*, North-Holland, Amsterdam, 1978.
- [8] R. CLAYTON AND B. ENGQUIST, *Absorbing boundary conditions for acoustic and elastic wave calculations*, Bull. Seismol. Soc. Amer., 67 (1977), pp. 1529–1540.
- [9] B. DESPRÉS, *Domain decomposition method and the Helmholtz problem*, in Mathematical and Numerical Aspects of Wave Propagation Phenomena, G. Cohen, L. Halpern, and P. Joly, eds., Philadelphia, 1991, SIAM, pp. 44–52.

- [10] J. DOUGLAS, JR., J. L. HENSLEY, AND J. E. ROBERTS, *An alternating-direction iteration method for Helmholtz problems*, Appl. Math., 38 (1993), pp. 289–300.
- [11] J. DOUGLAS, JR., P. PAES LEME, J. ROBERTS, AND J. WANG, *A parallel iterative procedure applicable to the approximate solution of second order partial differential equations by mixed finite element methods*, Numer. Math., 65 (1993), pp. 95–108.
- [12] J. DOUGLAS, JR., J. E. SANTOS, AND D. SHEEN, *Approximation of scalar waves in the space-frequency domain*, Math. Models Methods Appl. Sci., 4 (1994), pp. 509–531.
- [13] M. DRYJA AND O. WIDLUND, *Some recent results on Schwarz type domain decomposition algorithms*, in Domain Decomposition Methods in Science and Engineering, A. Quarteroni, J. Periaux, Y. Kuznetsov, and O. Widlund, eds., vol. 157 of Contemporary Mathematics, Philadelphia, 1994, SIAM, pp. 53–61.
- [14] S. EISENSTAT, H. ELMAN, AND M. SCHULTZ, *Variational iterative methods for non-symmetric systems of linear equations*, SIAM J. Numer. Anal., 20 (1983), pp. 345–357.
- [15] H. C. ELMAN AND O. G. ERNST, *Numerical experiences with a Krylov-enhanced multigrid solver for exterior Helmholtz problems*, in Mathematical and Numerical Aspects of Wave Propagation, Philadelphia, PA, 2000, SIAM, pp. 797–801.
- [16] V. FABER AND T. MANTEUFFEL, *Necessary and sufficient conditions for the existence of a conjugate gradient method*, SIAM J. Numer. Anal., 21 (1984), pp. 352–362.
- [17] R. W. FREUND, *Conjugate gradient-type methods for linear systems with complex symmetric coefficient matrices*, SIAM J. Sci. Stat. Comput., 13 (1992), pp. 425–448.
- [18] W. JOUBERT AND D. YOUNG, *Necessary and sufficient conditions for the simplification of the generalized conjugate-gradient algorithms*, Linear Algebra Appl., 88/89 (1987), pp. 449–485.
- [19] S. KIM, *A parallelizable iterative procedure for the Helmholtz problem*, Appl. Numer. Math., 14 (1994), pp. 435–449.
- [20] —, *Parallel multidomain iterative algorithms for the Helmholtz wave equation*, Appl. Numer. Math., 17 (1995), pp. 411–429.
- [21] —, *Domain decomposition iterative procedures for solving scalar waves in the frequency domain*, Numer. Math., 79 (1998), pp. 231–259.

- [22] —, *On the use of rational iterations and domain decomposition methods for solving the Helmholtz problem*, Numer. Math., 79 (1998), pp. 529–552.
- [23] S. KIM AND S. KIM, *Multigrid simulation for high-frequency solutions of the Helmholtz problem in heterogeneous media*, SIAM J. Sci. Comput., 24 (2002), pp. 684–701.
- [24] S. KIM AND M. LEE, *Artificial damping techniques for scalar waves in the frequency domain*, Computers Math. Applic., 31, No. 8 (1996), pp. 1–12.
- [25] S. KIM, C. SHIN, AND J. KELLER, *High-frequency asymptotics for the numerical solution of the Helmholtz equation*, Appl. Math. Letters, (2005). (in press).
- [26] P. LE TALLEC, *Domain decomposition methods in computational mechanics*, Comput. Mech. Advances, 1 (1994), pp. 121–220.
- [27] B. LEE, T. MANTEUFFEL, S. MCCORMICK, AND J. RUGE, *First-order system least-squares for the Helmholtz equation*, SIAM J. Sci. Comput., 21 (2000), pp. 1927–1949.
- [28] P. LIONS, *On the Schwarz alternating method III: a variant for nonoverlapping subdomains*, in Domain Decomposition Methods for Partial Differential Equations, T. Chan, R. Glowinski, J. Periaux, and O. Widlund, eds., Philadelphia, PA, 1990, SIAM, pp. 202–223.
- [29] L. MCINNES, R. SUSAN-RESIGA, D. KEYES, AND H. ATASSI, *Additive Schwarz methods with nonreflecting boundary conditions for the parallel computation of Helmholtz problems*, in Domain Decomposition Methods 10, J. Mandel, C. Farhat, and X.-C. Cai, eds., vol. 218 of Contemporary Mathematics, Providence, RI, 1998, American Mathematical Society, pp. 325–333. Proceedings of the Tenth International Conference on Domain Decomposition Methods, August 10-14, 1997, Boulder, CO.
- [30] Y. SAAD AND M. SCHULTZ, *GMRES: A generalized minimal residual algorithm for solving nonsymmetric linear systems*, SIAM J. Sci. Stat. Comput., 7 (1986), pp. 856–869.
- [31] V. SHAIUROV AND E. OGORODNIKOV, *Some numerical methods of solving Helmholtz wave equation*, in Mathematical and Numerical Aspects of Wave Propagation Phenomena, G. Cohen, L. Halpern, and P. Joly, eds., Philadelphia, 1991, SIAM, pp. 73–79.
- [32] W. TANG, *Generalized Schwarz splittings*, SIAM J. Sci. Stat. Comput., 13 (1992), pp. 573–595.